Journal of New Materials for Electrochemical Systems 18, 043-048 (2015)

Composite Supercapacitor Electrodes by Electrodeposition of MnO_2 on MWCNT Felt Directly Grown on Aluminum

Reza Kavian[1], Antonello Vicenzo[1,*] and Massimiliano Bestetti[1]

Politecnico di Milano - Dipartimento di Chimica, Materiali e Ingegneria Chimica "Giulio Natta" - Via Mancinelli 7, 20131 Milano, Italy

Received: September 20, 2014, Accepted: December 23, 2014, Available online: February 11, 2015

Abstract: *Manganese oxide \ carbon nanotube (CNT) thin film electrodes were fabricated by direct growth of a carbon nanotube layer on aluminum substrate (i.e. a commercially viable material for use as current collector) by chemical vapor deposition, in the presence of an electrochemically deposited thin film nickel catalyst, followed by anodic electrodeposition of MnO_2. A proof of concept of this approach is demonstrated showing that the fabrication process, even in its simplest and unsophisticated implementation –notably without any deliberate effort to control the CNT growth arrangement and consequently the composite microstructure– allows the preparation of MnO_2/CNT/Al prototype electrodes having almost a three-fold increase in capacitance compared to MnO_2/Ni electrodes and, more significantly, comparing favorably with composite electrodes of similar design and fabrication. MnO_2/CNT/Al electrodes ensured also improved cyclic stability compared to the reference case of MnO_2/Ni electrodes. The proposed scheme is an effective procedure for the fabrication of thin film composite MnO_2/CNT/Al electrodes, which may be amenable to significant improvements by tailoring thickness and microstructure of the CNT scaffold and manganese oxide film. Furthermore, a similar process scheme, may be proposed for the fabrication of active electrodes of different scopes with a proper choice of the substrate.*

Keywords: manganese oxide, carbon nanotubes, direct growth, composite electrode film, metal substrate

1. INTRODUCTION

Design and fabrication of composite electrode materials is a research area of high potential impact on a variety of applications, particularly in, but not limited to, the area of electrochemical energy storage and conversion, such as electrical double layer capacitors (EDLC). Diverse carbon materials have been used for supercapacitor electrode fabrication, while conductive polymers and metal oxides have been considered for their pseudo-capacitive behavior [1], each kind of material having its own advantages and disadvantages [2-3]. Accordingly, among new directions being investigated towards the enhancement of EDLCs performance –namely, for boosting energy density preserving high power density– a promising approach is the fabrication of composite electrodes and the development of hybrid systems [4]. In particular, the combination in a single electrode of materials exhibiting complementary charge storage mechanisms has been widely explored [5]. In this respect, an obvious combination is that between a carbon based material and a metal oxide displaying pseudo-capacitive behavior [6]. Among the metal oxides, manganese oxide MnO_2 is considered as a promising material for the next generation of EDLCs because of its low cost, environmentally friendly nature, and outstanding specific capacitance, though high electrical resistivity and comparatively low cycle life –which is common to most oxide materials considered for same applications however, with the only notable exception of RuO_2 [1]– pose serious concern for its successful implementation in commercial devices [7-11]. Consequently, the synthesis of nanostructured, porous MnO_2 materials has been actively studied to improve the electrochemical performance [12]. In particular, it has been reported that the thin film form of MnO_2 electrode has the highest specific capacitance, dropping dramatically with the increase of thickness [10, 13]. In the light of this intrinsic limitation, a strategy towards the rationale exploitation of the electrochemical activity of the material has been the preparation of composite electrode by either powder based process, with incorporation of an electrical conductivity enhancer and a binder, or by deposition / precipitation of MnO_2 onto a conductive porous matrix, such as a carbon nanotube (CNT) layer [14]. The main focus has been obviously the enhancement of

*To whom correspondence should be addressed: Email: antonello.vicenzo@polimi.it
Phone: +39-02-23993140 ; Fax: +39-02-23993180

the surface area of the oxide by a suitable choice and preparation of the conductive scaffold serving as the support, also in the attempt to achieve a low electrical resistance of the composite and minimize the drawbacks of the low electric conductivity of MnO_2 [15].

A variety of different methods have been explored for the preparation of manganese oxides [12]. In particular, the electrochemical deposition (ECD) of MnO_2 has been reported using either steady state [16-19] or transient techniques [17,20], under current or potential control. Moreover, varying combinations of synthesis, deposition methods and type of substrate, including its modification for the enhancement of surface area, have been probed for the fabrication of MnO_2 electrodes [12]. An even wider variability of approaches has been put forward for the fabrication of carbon-MnO_2 composite electrodes [21-24], leading to variable design and architectures [5].

However, most of the diverse procedures that have been proposed for the fabrication of CNT based composite electrodes suffer from an intrinsic limitation, namely an expectedly weak and high resistance interface between the active material and the substrate, due to the widespread use of the transfer technique and possibly also of a binder [12,25]. Direct growth of CNTs on metals has been studied over recent years offering an in principle straightforward processing solution to overcome this issue [25]. However, the choice of the substrate material as well as the detail processing procedure are still actively studied, in the search of effective and feasible solutions. In particular, significant and reliable results have been achieved in recent years using aluminum foil as the substrate for direct growth of CNTs [26-29], whilst on the other hand doubt may be cast on the suitability of other materials for the same purpose, including stainless steel –a widely used current collector in commercial EDLC– in view of its susceptibility to carburization [30].

In the present work, a fabrication procedure has been evaluated in the attempt to conceive a relatively simple and scalable manufacturing process, which general objective is the preparation of CNT-based metal (Al) supported electrodes loaded with the active material. Accordingly, MnO_2/CNT/Al thin film electrodes were fabricated by ECD of MnO_2 on CNT layers directly grown on an Al substrate by catalytic chemical vapor deposition (CVD). A schematic of the process steps involved in the fabrication of the electrodes is given in Fig. 1. The proof of concept of the process is demonstrated based on the study of the capacitive behavior of the electrodes.

The distinctive feature of the present approach is the direct growth of the CNT scaffold on an aluminum substrate, which is obviously a commercially viable solution for supercapacitor electrodes, notably compared to such substrate materials as tantalum [21,31] silicon [32,33], carbon fabric [34], that were previously used in similar fabrication schemes. Accordingly, the main purpose of this study was to demonstrate the feasibility of an industrially viable process for the fabrication of such electrodes, using comparatively unsophisticated procedure: namely, the electrodeposition of a nickel thin film as the catalyst for CNT growth; a simple atmospheric CVD process for the deposition of the CNT layer on Al using ethylene as the carbon precursor (a process relatively little studied in the literature, see [29] and reference therein); and, finally, the electrodeposition of the oxide from a dilute acetate electrolyte.

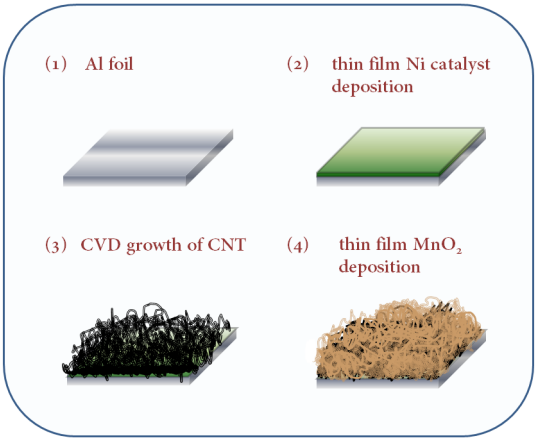

Figure 1. Schematic of the proposed process for the preparation of composite MnO_2/CNT/Al electrode.

2. EXPERIMENTAL

MnO_2 films were deposited from 0.01 M $Mn(CH_3COO)_2$ (purum, ≥99%, Sigma-Aldrich) electrolyte, under stirring provided by a magnetically driven bar at a speed of 500 rpm and room temperature. The deposition was performed by a potential ramp technique (in the following referred to as potentiodynamic polarization technique) scanning the potential at 1 mV s^{-1} over the range 0.4-1.1 V. A platinum mesh, as the counter electrode, and a saturated calomel electrode (SCE), as the reference electrode, were used throughout this work. High purity electroformed nickel sheets served as substrate for the preparation of single layer MnO_2 electrode. Before ECD, the Ni substrate was washed with acetone and distilled water, activated by immersion in 0.1 M HCl (ACS, 37%, Sigma-Aldrich), then thoroughly rinsed with distilled water, and finally dried in a stream of hot air. Al thin foils (99.999% purity) coated with a multi-walled CNT layer formed by CVD were used as the substrate for the fabrication of two-layer electrodes. The amount of MnO_2 deposited was determined from the weight difference of the sample before and after deposition, as measured using a microbalance (Sartorius ART 692 CP) with an accuracy of 1 μg.

The CVD reactor used for the deposition of the CNT layer was a vertical quartz tube heated in a temperature controlled furnace (Carbolite, Endotherm VST 24-16). Al strips coated with an ECD thin film of Ni catalyst was placed vertically on a porous type P2 (pore sizes 40-100 mm; ISO 4793-1980) gas distributor in the quartz reactor (Ø 2.28 cm). Ethylene (C_2H_4) was used as carbon source. Initially, a mixture of H_2/N_2 (N_2 20 sccm, H_2 20 sccm) was fed to the reactor, and the furnace temperature was increased at 15°C min^{-1} rate up to 600°C. As the temperature was stabilized, the flow rate of the C_2H_4 reactant was adjusted to the desired value (20 sccm) and fed to the reactor together with the H_2/N_2 mixture for 10 min to grow CNTs. Finally, the reactor was flushed with nitrogen gas and cooled down to room temperature. More detail can be found in a previous paper [26]. The morphology of the MnO_2 and MnO_2/CNT electrodes was observed by atomic force microscopy (AFM), using an NT-MDT Solver Pro instrument operated in contact mode, and scanning electron microscopy (SEM, Zeiss EVO 50

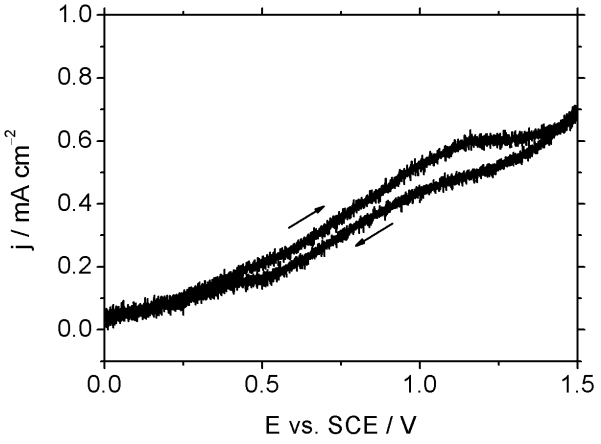

Figure 2. Cyclic linear polarization curve (1 mV s^{-1}) at nickel substrate in 0.01 M $Mn(CH_3COO)_2$ solution at 25°C.

EP). The crystal structure of manganese oxide was assessed by X-ray diffraction (XRD, Philips PW 1830), acquiring XRD spectra over the 2θ range 30–70°. The electrochemical behavior of the electrodes was investigated in 0.1 M Na_2SO_4 electrolyte by cyclic voltammetry (CV) using an Amel Mod. 7050 potentiostat. A three-electrode configuration cell was used, consisting of an MnO_2/Ni or Al/CNT/MnO_2 sample (working electrode, 0.64 cm^2 area), a platinum mesh (counter electrode) and an SCE (saturated calomel electrode, reference electrode). CV curves were recorded between 0 and 1 V at 20, 50 and 100 mV s^{-1} scanning rate, and room temperature. The specific capacitance was calculated from the voltammetric charge integrated over the potential scanning range, according to the equation $C=Q/(\Delta E \cdot m)$, where C / F g^{-1} is the specific capacitance, Q / C is the charge, ΔE / V is the scanning potential range, and m / g is the mass of active material.

3. RESULTS AND DISCUSSION

Fig. 2 shows the cyclic linear polarization curve recorded at Ni electrode in the $Mn(CH_3COO)_2$ 0.01 M electrolyte at scan rate of 1 mV s^{-1} and 25°C. According to the potential-pH diagram of the Mn-H_2O system, at pH close to 7 the formation of MnO_2 by the electrochemical oxidation of Mn(II) should occur in a relatively wide potential range, starting at about 0.4 V. During the forward anodic scan, a progressive onset of the oxidation of Mn(II) species is apparent, with an almost linear increase of the c.d. over most of the scanned potential range up to 1.1 V, where the c.d. reaches a *plateau* value of 0.6 mA cm^{-2}. With further increase of potential above about 1.25 V, the c.d. takes on a slowly increasing trend, preluding to the onset of oxygen evolution at about 1.4 V. During the backward scan, no major changes in the trace of the curve can be noticed, probably also as a consequence of increased surface area compensating for a lower expected electron transfer rate at the freshly deposited oxide. Since the oxidation rate reaches a limiting value in the potential region corresponding to the c.d. plateau, the deposition of MnO_2 was performed by scanning the potential from 0.4 to 1.1 V at 1 mV s^{-1} and 25°C, obtained an oxide mass load of about 0.16 mg cm^{-2}.

The crystal structure of MnO_2 films deposited on nickel was

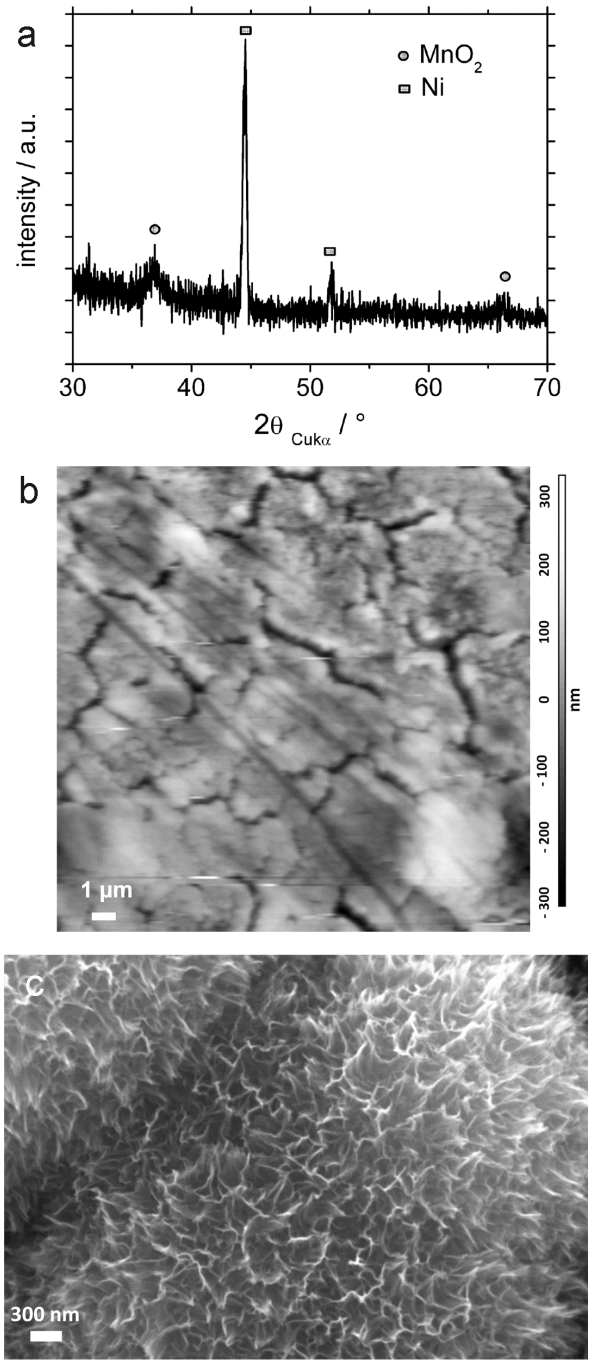

Figure 3. (a) XRD pattern, (b) AFM and (c) SEM surface images of MnO_2/Ni deposited from 0.01 M $Mn(CH_3COO)_2$ electrolyte by potentiodynamic polarization (0.4-1.1 V, 1 mV s^{-1}), at room temperature.

investigated by XRD. In the XRD pattern of Fig. 3-(a), the peaks at 2θ about 36.8° and 66.3 can be attributed to the (100) and (110) reflection of the hexagonal MnO_2 phase, while the other peaks belong to the nickel. The crystal size of the manganese oxide is in the range of 10 nm, as deduced by applying the Scherrer's equation

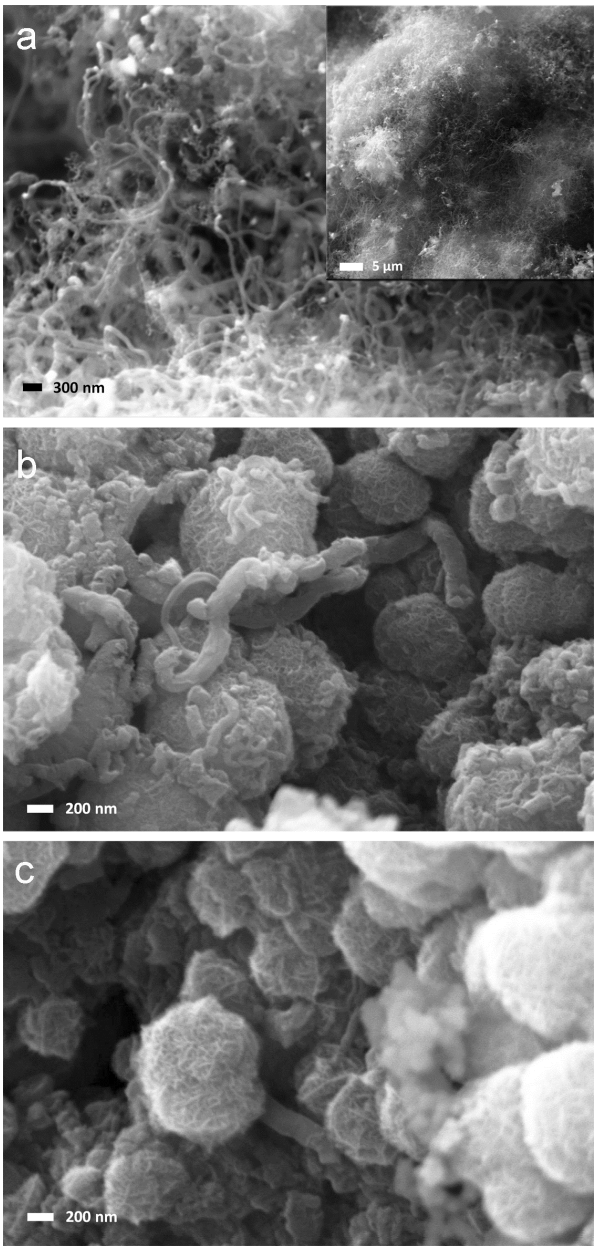

Figure 4. SEM micrographs of: (a) CNT layer directly grown on aluminum, and (b), (c) of MnO_2/CNT/Al composite electrode.

to the (100) peak.

As shown by the AFM image in Fig. 3-(b) , the MnO_2 film has seemingly a cracked mud like morphology, consisting of large islands –actually aggregates of globular grains– separated by grooves and cracks. By single line scanning across various grooves, the depth of these discontinuities was found to be mostly in the range of 250 to 350 nm. The morphology of as–prepared oxide films on Ni was further characterized by SEM analysis, as shown in Fig. 3-(c). The oxide consists of highly interconnected thin petal-like crystallites, forming relatively large grains in the shape of globular features. This morphology appears different from that of MnO_2 thin films deposited from sulfate electrolytes, which typically consists of thin lathe-like crystallites arranged in globules of variable size, further merged into larger and irregular features [35-37]. Nonetheless, similarly to the latter, the crystallites are very thin, less than 20 nm, and of variable length, forming a dense array of nano-ridges.

Multi-walled CNTs were grown on Al substrate with a thin film Ni catalyst layer by CVD, as described in a previous work [26]. The amount of CNT deposited per unit area of the substrate was about 0.4 mg cm^{-2}. Accordingly, Al/CNT had a relatively high value of specific capacitance, about 60 F g^{-1} at 20 mV s^{-1} in Na_2SO_4 0.1 M (not shown here). As shown in Fig. 4-(a), the CNT layer consists of dense bundles of nanotubes (see inset of Fig. 4-(a)) with diameter in the range from 50 to 100 nm and several micrometers in length, though large diameter fibers and other nanostructures can also be observed in the high magnification image, as expected in view of the low growth temperature, see also [26] for further detail.

Manganese oxide was deposited on Al/CNT samples by potentiodynamic polarization at 1 mV s^{-1}, scanning the potential from 0.4 to 1.1 V, obtaining a unit oxide mass in the range from 0.10 to 0.12 mg cm^{-2}. Fig. 4-(b) and Fig. 4-(c) show the appearance of the Al/CNT/MnO_2 composite electrode: apparently, the CNT layer was completely covered by manganese oxide crystals forming agglomerates of quasi-spherical particles, with size in the range from about 0.1 to 1 µm. Occasionally, fine CNTs can be seen to sprout from the particles, thus suggesting that the latter may grow by coalescence of MnO_2 precipitates wrapping individual nanotubes and progressively stuffing the native porosity of the bundles. Very distinctly, on the other hand, large diameter nanotubes and likely fibers can be spotted at the surface, which appear to be completely enveloped by the precipitated oxide.

As a proof of principle of the application potential of the electrodes, we performed cyclic voltammetry for the assessment of electrode capacitance, in an aqueous 0.1 M Na_2SO_4 electrolyte kept at room temperature, scanning the potential in the range 0.0–1.0 V vs SCE, at varying scan rate (20, 50 and 100 mV s^{-1}). CV curves at the MnO_2/Ni (a) and the MnO_2/CNT/Al electrodes are shown on the left column of Fig. 5-(a) and Fig. 5-(b), respectively.

At the scan rate of 20 and 50 mV s^{-1}, the shape of the CV curves recorded at MnO_2/Ni electrodes suggests a close to ideal capacitive behavior of the MnO_2 thin film under charging conditions, seemingly ensuring the redox transformation for a relatively large fraction of the electrode material. On the other hand, though as expected, cyclic voltammetry reveals a relatively long time constant for charge and discharge processes, probably related to both the limited conductivity of the oxide and charge transfer resistance for the surface redox reaction. Actually, as the scan rate is increased to 100 mV s^{-1}, a distinct change is seen in the shape of the voltammogram, revealing a sloping trend for the charging current, which is expectedly due to the inherently low power capability of the oxide thin film. A progressive and fast activation of the electrode is also apparent with cycling (indicated by the arrow), confirming the rate sensitivity of the material to charging at the highest scan rate. The specific capacitance of MnO_2/Ni thin film electrodes was 140 F g^{-1} (at scan rate of 20 mV s^{-1}) and decreased to about 105 F g^{-1} and 80 F g^{-1} at 50 and 100 mV s^{-1}, respectively. Cyclic voltammetry was also performed to characterize the capacitive behavior of the MnO_2/CNT/Al electrodes, in the

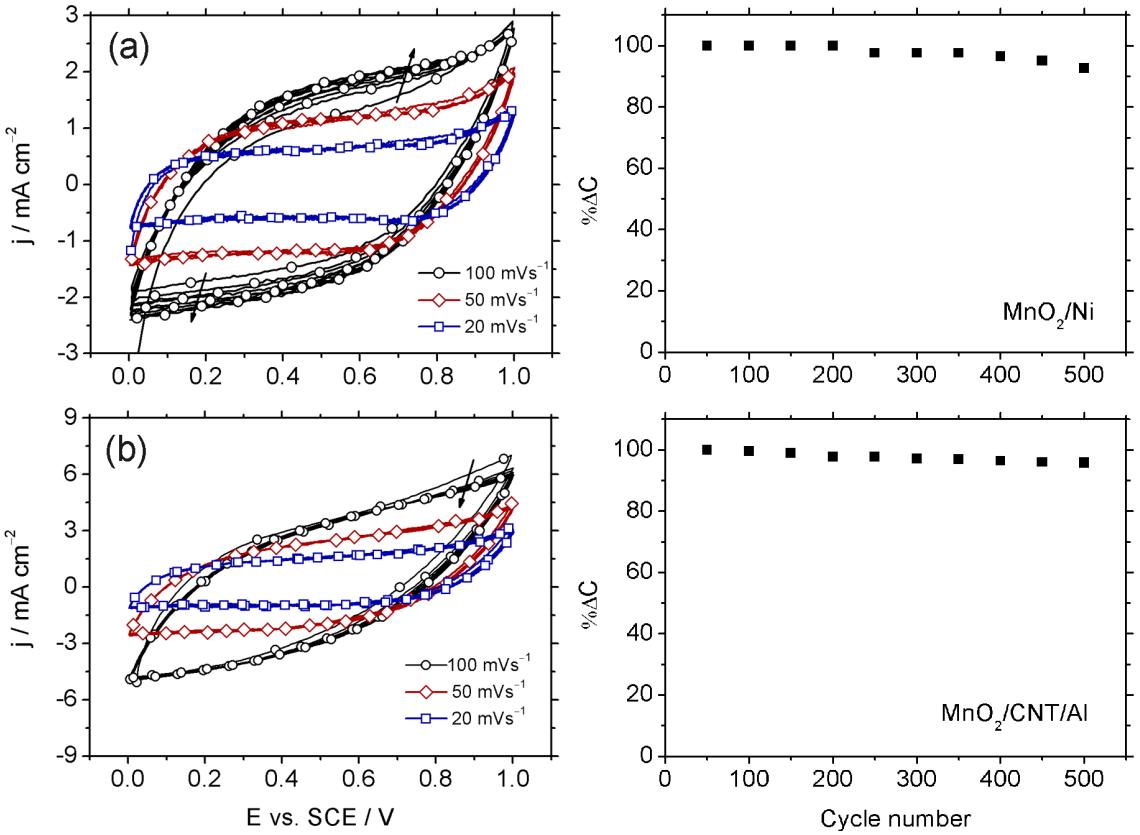

Figure 5. On the left column, CV curves at MnO_2/Ni (a) and MnO_2/CNT/Al (b) electrodes in Na_2SO_4 0.1 M at varying scan rate, as indicated; on the right, change of capacitance with cycling for MnO_2/Ni (a) and MnO_2/CNT/Al (b) electrodes, as indicated, in Na_2SO_4 0.1 M at 100 mV s^{-1} scan rate.

same conditions as for MnO_2/Ni electrodes. The specific capacitance of MnO_2/CNT/Al electrodes, based on the mass of oxide, was as high as 450 F g^{-1} at 20 mV s^{-1}, decreasing with scan rate to 320 and 230 F g^{-1}, at 50 and 100 mV s^{-1}, respectively.

A meaningful comparison of the performance of different supercapacitor electrodes is somehow elusive and may be misleading, due to the effects of even subtle differences in design and fabrication of the electrodes. However, the value of the specific capacitance can be regarded as a reasonably reliable, though rough, parameter for a comparative assessment of the relative efficacy of different processing routes, provided that the main experimental conditions, pertaining to both processing and testing, are close enough. Accordingly, the present result, namely a specific capacitance of 450 F g^{-1} at 20 mV s^{-1} (resulting in a specific current plateau during the discharge semi-cycle of about 10 A g^{-1}) for an oxide mass per unit area in the range of 0.10 to 0.12 mg cm^{-2}, compares quite favorably to the performance of MnO_2 coated CNT array electrodes, as reported for example in [32] (400 F g^{-1} at 10 A g^{-1} for an oxide mass per unit area of 0.05 mg cm^{-2} in Na_2SO_4 0.5 M electrolyte) and in [38] (about 500 F g^{-1} at 20 mV s^{-1} in Na_2SO_4 0.2 M electrolyte, but with an oxide load of the order of 0.01 mg cm^{-2}; it should also be stressed that in the latter work, CNT array electrodes were fabricated using a complex vapor phase deposition system, including two sputtering target and a cathode for plasma enhanced CVD). On the other hand, but expectedly, the performance of the MnO_2/CNT/Al electrode is inferior to that of electrode with tailored architectures, such as long vertically aligned CNT array decorated with MnO_2 nanoparticles [21], which however stands as a rather unique case, and obviously relies on a more sophisticated fabrication process.

Notwithstanding the practical relevance of process complexity and costs, it is however noteworthy the finding that the MnO_2/CNT composite electrode of the present work might achieve similar performance in term of specific capacitance as that of MnO_2 coated CNT array electrodes [32,38], having definitely a much more refined structure (namely, MnO_2 conformally coated arrays of aligned CNTs).

The electrochemical cycling behaviour was assessed by performing CV over the same potential range as above and in the same solution, at scan rate of 100 mV s^{-1}. The percentage change of capacitance with cycle number is shown by the graphs on the right column of Fig. 5(a) and Fig. 5(b), respectively for the MnO_2/Ni and MnO_2/CNT/Al electrodes. The specific capacitance decrease observed for MnO_2/Ni electrodes is about 7.4% after 500 cycles; for MnO_2/CNT/Al electrodes, the loss of capacitance over 500 cycles amounts to about 4.3%. Among the factors that may be responsible for decreasing capacitance of the electrodes, structural modification, active material dissolution and increasing electrode

resistance are the most significant [39]. In the absence of direct evidence concerning the electrode degradation, the latter may be the most likely mechanism responsible for the observed behavior. In fact, the dissolution of the active material can be ruled out as a degrading factor, since the surface area of MnO_2/CNT/Al is obviously higher that of MnO_2/Ni electrode, and therefore it would produce the opposite effect; besides, any structural modification due to intercalation and deintercalation of ionic species, should affect in a similar way the thin film of MnO_2 and possibly have a stronger effect on the composite electrode, for the same reason as above.

4. CONCLUSIONS

MnO_2/CNT/Al composite electrodes were produced by using thin film deposition techniques, namely CVD as the method for the direct growth of CNTs on an aluminum current collector, in the presence of a thin film nickel catalyst, and anodic electrodeposition for the formation of the MnO_2 layer. The composite electrodes were characterized for their capacitive behavior by cyclic voltammetry, showing a much higher capacitance compared to MnO_2/Ni electrodes, and also a significant improvement in the cyclic stability of the capacitance. The direct growth of CNTs on an aluminum current collector is the key aspect of this fabrication process, and in principle its main advantage compared to other procedures of forming CNT films on metal substrates. The designed process is expected to be amenable to further improvements by carefully optimizing the operating parameters and enabling a degree of control over the electrode architecture.

Notwithstanding the example application considered in the present work, this fabrication approach is very promising and should be considered in a larger perspective, as a viable process for the fabrication of high surface area electrodes, of potential interest to a wide range of applications.

REFERENCES

[1] Conway BE., Electrochemical Supercapacitors - Scientific Fundamentals and Technological Applications Plenum Press, New York, 1999.
[2] E. Frackowiak, F. Beguin, Carbon, 39, 937 (2001).
[3] S. Ghosh, O. Inganas, Adv. Mater., 11, 1214 (1999).
[4] Y. Zhang, H Feng, X. Wu, L. Wang, A. Zhang, T. Xia, H. Dong, X. Li, L. Zhang, Int. J. Hydrogen Energy, 34, 4889 (2009).
[5] M. Zhi, C. Xiang, J. Li, M. Li and N. Wu, Nanoscale, 5, 72 (2013).
[6] J.P. Zheng, Electrochem. Solid-State Lett., 2, 359 (1999).
[7] H.Y. Lee, J.B. Goodenough, J. Solid State Chem., 144, 220 (1999).
[8] C.C. Hu, T.W. Tsou, Electrochem. Commun., 4, 105 (2002).
[9] M. Toupin, T. Brousse, D. Belanger, Chem. Mater., 14, 3946 (2002).
[10]M. Toupin, T. Brousse, D. Belanger, Chem. Mater., 16, 3184 (2004).
[11]R.N Reddy, R.G. Reddy, J. Power Sources, 124, 330 (2003).
[12]W. Wei, X. Cui, W. Chen and D.G. Ivey, Chem. Soc. Rev., 40, 1697 (2011).
[13]S.C. Pang, M.A. Anderson, T.W. Chapman, J. Electrochem. Soc., 147, 444 (2000).
[14]S.-L. Chou, J.-Z. Wang, S.-Y. Chew, H.-K. Liu, S.-X. Dou, Electrochem. Commun., 10, 1724 (2008).
[15]D.B. Rogers, R.D. Shannon, A.W. Sleight and J.L. Gillson, Inorg. Chem., 8, 841 (1969).
[16]D. Tench, L.F. Warren, J. Electrochem. Soc., 130, 869 (1983).
[17]C.-C. Hu, C.-C. Wang, J. Electrochem. Soc., 150, A1079 (2003).
[18]G.J. Moore, R. Portal, A.L.G. La Salle, D. Guyomard, J. Power Sources, 97, 393 (2001).
[19]C.-C. Hu, T.W. Tsou, Electrochim. Acta., 47, 3523 (2002).
[20]M.S. Wu, Appl. Phys. Lett., 87, 153102 (2005).
[21]H. Zhang, G. Cao, Z. Wang, Y. Yang, Z. Shi and Z. Gu, Nano Lett., 8, 264 (2008).
[22]Y. Wang, H. Liu, X. Sun and I. Zhitomirsky, Scr. Mater., 61, 1079 (2009).
[23]H. Xia, Y. Wang, J. Lin and L. Lu, Nanoscale Res. Lett., 7, 33 (2012).
[24]R. Amade, E. Jover, B. Caglar, T. Mutlu, E. Bertran, J. Power Sources, 196, 5779 (2011).
[25]N.S.A. Manaf, M.S.A. Bistamam and M.A. Azam, ECS J. Solid State Sci. Technol., 2, M3101 (2013).
[26]R. Kavian, A. Vicenzo, M. Bestetti, J. Mater. Sci., 46, 1487 (2011).
[27]R. Reit, J. Nguyen, W.J. Ready, Electrochim. Acta, 91, 96 (2013).
[28]S. Dörfler, I. Felhösi, T. Marek, S. Thieme, H. Althues, L. Nyikos, S. Kaskel, J. Power Sources, 227, 218 (2013).
[29]F. Zhao, A. Vicenzo, M. Hashempour, M. Bestetti, Electrochim. Acta, 150, 35 (2014).
[30]M. Hashempour, A. Vicenzo, F. Zhao and M. Bestetti, Mater. Charact., 92, 64 (2014).
[31]G. Mo, Y. Zhang, W. Zhang, J. Ye, Electrochim. Acta, 113, 373 (2013).
[32]D.-D. Zhao, Z. Yang, E.S.-W. Kong, C.-L. Xu, Y.-F. Zhang, J. Solid State Electrochem., 15, 1235 (2011).
[33]J. Liu, J. Essner and J. Li, Chem. Mater. 22, 5022 (2010).
[34]P. Lv, P. Zhang, Y. Feng, Y. Li, W. Feng, Electrochim. Acta, 78, 515 (2012).
[35]T. Shinomiya, V. Gupta, N. Miura, Electrochim. Acta, 51, 4412 (2006).
[36]M.P. Owen, G.A. Lawrance, S.W. Donne, Electrochim. Acta, 52, 4630 (2007).
[37]Y.-C. Chen, Y.-K. Hsu, Y-G. Lin, Y.-K. Lin, Y.-Y. Horn, L.-C. Chen, K.-H. Chen, Electrochim. Acta, 56, 7124 (2011).
[38]R. Amade, E. Jover, B. Caglar, T. Mutlu, E. Bertran, J. Power Sources, 196, 5779 (2011).
[39]D. Bélanger, T. Brousse and J.W. Long, Electrochem. Soc. Interface, 17, 34 (2008).